NASA/TM—2012-217700

Ice Particle Transport Analysis With Phase Change for the E^3 Turbofan Engine Using LEWICE3D Version 3.2

Colin S. Bidwell
Glenn Research Center, Cleveland, Ohio

September 2012

NASA STI Program . . . in Profile

Since its founding, NASA has been dedicated to the advancement of aeronautics and space science. The NASA Scientific and Technical Information (STI) program plays a key part in helping NASA maintain this important role.

The NASA STI Program operates under the auspices of the Agency Chief Information Officer. It collects, organizes, provides for archiving, and disseminates NASA's STI. The NASA STI program provides access to the NASA Aeronautics and Space Database and its public interface, the NASA Technical Reports Server, thus providing one of the largest collections of aeronautical and space science STI in the world. Results are published in both non-NASA channels and by NASA in the NASA STI Report Series, which includes the following report types:

- TECHNICAL PUBLICATION. Reports of completed research or a major significant phase of research that present the results of NASA programs and include extensive data or theoretical analysis. Includes compilations of significant scientific and technical data and information deemed to be of continuing reference value. NASA counterpart of peer-reviewed formal professional papers but has less stringent limitations on manuscript length and extent of graphic presentations.

- TECHNICAL MEMORANDUM. Scientific and technical findings that are preliminary or of specialized interest, e.g., quick release reports, working papers, and bibliographies that contain minimal annotation. Does not contain extensive analysis.

- CONTRACTOR REPORT. Scientific and technical findings by NASA-sponsored contractors and grantees.

- CONFERENCE PUBLICATION. Collected papers from scientific and technical conferences, symposia, seminars, or other meetings sponsored or cosponsored by NASA.

- SPECIAL PUBLICATION. Scientific, technical, or historical information from NASA programs, projects, and missions, often concerned with subjects having substantial public interest.

- TECHNICAL TRANSLATION. English-language translations of foreign scientific and technical material pertinent to NASA's mission.

Specialized services also include creating custom thesauri, building customized databases, organizing and publishing research results.

For more information about the NASA STI program, see the following:

- Access the NASA STI program home page at *http://www.sti.nasa.gov*

- E-mail your question to *help@sti.nasa.gov*

- Fax your question to the NASA STI Information Desk at 443–757–5803

- Phone the NASA STI Information Desk at 443–757–5802

- Write to:
  STI Information Desk
  NASA Center for AeroSpace Information
  7115 Standard Drive
  Hanover, MD 21076–1320

NASA/TM—2012-217700

Ice Particle Transport Analysis With Phase Change for the E^3 Turbofan Engine Using LEWICE3D Version 3.2

Colin S. Bidwell
Glenn Research Center, Cleveland, Ohio

Prepared for the
Atmospheric Space Environments Conference
sponsored by the American Institute of Aeronautics and Astronautics
New Orleans, Louisiana, June 25–28, 2012

National Aeronautics and
Space Administration

Glenn Research Center
Cleveland, Ohio 44135

September 2012

Acknowledgments

The author would like to thank Joseph Veres, Philip Jorgenson and Russell Claus of the NASA Glenn Research Center, Cleveland, Ohio for contributing the flow solution for the E^3 compressor and for aid in interpreting turbomachinery flow and particle transport physics. The NASA Aviation Safety Program, Atmospheric Environment Safety Technologies Project supported this work.

This work was sponsored by the Fundamental Aeronautics Program at the NASA Glenn Research Center.

Level of Review: This material has been technically reviewed by technical management.

Available from

NASA Center for Aerospace Information
7115 Standard Drive
Hanover, MD 21076–1320

National Technical Information Service
5301 Shawnee Road
Alexandria, VA 22312

Available electronically at http://www.sti.nasa.gov

Ice Particle Transport Analysis With Phase Change for the E^3 Turbofan Engine Using LEWICE3D Version 3.2

Colin S. Bidwell
National Aeronautics and Space Administration
Glenn Research Center
Cleveland, Ohio 44135

Abstract

Ice Particle trajectory calculations with phase change were made for the Energy Efficient Engine (E^3) using the LEWICE3D Version 3.2 software. The particle trajectory computations were performed using the new Glenn Ice Particle Phase Change Model which has been incorporated into the LEWICE3D Version 3.2 software. The E^3 was developed by NASA and GE in the early 1980's as a technology demonstrator and is representative of a modern high bypass turbofan engine. The E^3 flow field was calculated using the NASA Glenn ADPAC turbomachinery flow solver. Computations were performed for the low pressure compressor of the E^3 for a Mach 0.8 cruise condition at 11,887 m assuming a standard warm day for ice particle sizes of 5, 20, and 100 μm and a free stream particle concentration of 0.3 g/m^3. The impingement efficiency results showed that as particle size increased average impingement efficiencies and scoop factors increased for the various components. The particle analysis also showed that the amount of mass entering the inner core decreased with increased particle size because the larger particles were less able to negotiate the turn into the inner core due to particle inertia. The particle phase change analysis results showed that the larger particles warmed less as they were transported through the low pressure compressor. Only the smallest 5 μm particles were warmed enough to produce melting and the amount of melting was relatively small with a maximum average melting fraction of 0.836. The results also showed an appreciable amount of particle sublimation and evaporation for the 5 μm particles entering the engine core (22 percent).

Introduction

Over the last several years work has been ongoing to develop tools to analyze aircraft configurations subjected to High Ice Water Content (HIWC) conditions (Refs. 1 to 2). The HIWC environment contains conditions outside of the FAA Appendix C (Ref. 3) Certification Envelope. The HIWC environment contains large ice or mixed phase particles (>50 μm) in very high concentrations (~10 g/m^3) up to very high altitudes (~40000 ft). This HIWC environment has been responsible for many engine anomalies including engine roll backs and shutdowns (Ref. 1). Work is underway to quantify the HIWC environment and to develop ground test facilities and computational tools to assess the sensitivity of various engines to the HIWC environment. New certification rules, which will require aircraft to fly safely through these conditions, are on the horizon. It is anticipated that these new rules will generate new requirements for aircraft ice protection system design and certification and for the tools which aid in these processes. Icing computational tools, which have been successfully used in the design and certification of aircraft subject to the current FAA Appendix C icing environments, show great promise in their ability to analyze aircraft systems subject to the HIWC environment.

The development of icing computational analysis tools which produce sufficiently accurate results in a reasonable amount of computational time for turbomachinery flows has been a major challenge (Refs. 4 to 6). The use of unsteady tools to simulate the flow and particle transport in the highly time dependent turbomachinery flows was seen as impractical and as possibly unnecessary. For this reason a methodology was developed at NASA Glenn which uses the steady flow assumption commonly used in turbomachinery design tools. These methods typically model blade rows as a single blade with

circumferential symmetry and circumferentially averaged inflow and outflow boundary conditions which are generated from neighboring blade rows. These methods typically march through the turbomachinery calculating steady flow for each blade using the upstream blade outflow boundary data and the downstream inflow boundary data for the inflow and outflow boundary conditions respectively. Several passes through the engine to achieve convergence are typically employed by these methods

The newly developed NASA Glenn "block-to-block" icing analysis method follows the same logic used in these steady flow turbomachinery design tools. Ice particle or water droplet transport properties and ice shape calculations are generated for each blade row using steady, single blade flow solutions and the outflow particle size, state, concentration, and velocity data from the upstream blade row as inflow data. The upstream blade outflow particle concentration, velocities, and state are circumferentially averaged before being passed to the downstream blade row as an inflow boundary condition. This "block-to-block" method was incorporated into the LEWICE3D Version 3.2 software. (Refs. 6 and 7).

The E^3 engine (Refs. 8 to 10) was selected as a test case for the newly developed "block-to-block" method incorporated into LEWICE3D Version 3.2. The E^3 was developed by NASA and GE in the early 1980's as a technology demonstrator. The engine was chosen because it is representative of a modern high bypass turbofan engine, the geometry and experimental data were publicly available and flow solutions were readily available.

Nomenclature

A	Area, m^2
D	Ice particle diameter, μm
E^3	Energy Efficient Engine
IGV	Inlet Guide Vane
LWC	Liquid Water Content, g/m^3
IR	Impingement Rate, g/s
T	Ice particle temperature, K
SF	Scoop Factor
V	Velocity, m/s
β	Impingement efficiency

Analytical Method

Grid and Flow Calculations

GRIDGEN was used to develop the three-dimensional grids for the geometry (Ref. 11). The ADPAC flow solver (Refs. 12 to 14) was used to generate the flow solution for the analysis. The ADPAC code is a three-dimensional, finite volume based, Reynolds Averaged Navier-Stokes flow solver. The code computes flows on complex propulsion system configurations using multi-block body fitted grids. The method employs a "mixing-plane" procedure to pass boundary condition data between grid blocks for the steady state flows. The code supports parallel computing and uses a Baldwin-Lomax based turbulence model.

LEWICE3D

The LEWICE3D ice accretion code was used for the ice particle trajectory calculations. This grid based code incorporates particle trajectory, heat transfer and ice shape calculation into a single computer program. The code can handle generic multi-block structured grid based flow solutions, unstructured grid based flow solutions, simple Cartesian grids with surface patches, and adaptive grids with surface

patches. The latter two methods allow the use of generic panel code input which, when combined with LEWICE3D, is a computationally efficient method for generating ice shapes. The code can handle overlapping and internal grids and can handle multiple planes of symmetry. Calculations of arbitrary streamlines and trajectories are possible. The code has the capability to calculate tangent trajectories and impingement efficiencies for single drops or drop distributions using area based collection efficiency methods. Ice accretions can be calculated at arbitrary regions of interest in either a surface normal or tangent droplet trajectory direction. The program can run on a variety of single processor and parallel computers, including Unix, Linux, and Windows (Microsoft Corporation) based systems.

Version 3.2 of the LEWICE3D software which incorporates several new features was used for the analysis. These features include a new particle splash and bounce algorithm, the Glenn Ice Particle Phase Change Model (Ref. 5) which tracks ice particle or water drop state, a geometry handling scheme which allows complex mirroring, transformation and relative motion of input grid blocks and a new algorithm which calculates block-to-block collection efficiencies and particle properties. These new additions enable users to analyze HIWC conditions and to calculate collection efficiency with water or ice particle phase change, splash and bounce effects through turbo-machinery.

Analysis

The E^3 analysis included the calculation of flow and ice particle transport properties. The results for the flow are presented along with particle analysis for 5, 20, and 100 μm ice particle sizes.

The grid structure used for the flow and particle analysis is shown in Figure 1. The grid contained 12 structured, abutted grid blocks with a total of 327,583 nodes. The steady, viscous flow solution was generated for a Mach 0.8 cruise condition at 11998 m assuming a standard warm day. Flow vectors along the centerline of the axi-symmetric solution are shown in Figure 2.

The LEWICE3D ice particle analysis required several cloud input conditions and modeling parameters. The ice particle analysis assumed a free stream relative humidity of 0 percent and a free stream particle concentration of 0.3 g/m^3. The ice particles were assumed to be completely frozen and at the ambient temperature of the surrounding air (229.3 K). A simple particle impact and bounce model was used for this analysis because no model exists for the bounce and breakup of ice crystals typical of the HIWC environment. The simple particle bounce model assumed no breakup and no deposition. This was considered to be a reasonable assumption for a completely frozen ice particle. A coefficient of restitution of 1.0 and a coefficient of dynamic friction of 0.0 were used for the impact particle reflection model which yielded a lossless impact. This model was employed for all particle impacts in the engine and hence there was no buildup of ice. The ice particles were transported from the free stream through the compressor and out the compressor exit boundaries. Impingement efficiencies are reported for various surfaces. These were the net values that impinged upon the surface and do not represent the amount of ice that accreted on the surface. The actual values of accretion for all surfaces were zero because of the impact model employed (no deposition). Due to the bouncing model employed (multiple reflection and no deposition) the net amount of impingement on the engine solid surfaces (i.e., walls, blades, spinners, splitter lips, etc.) will be higher than that entering the engine. The amount of mass exiting the engine through the exit boundaries will however equal the amount entering the engine. The values are merely reported to give the reader information as to the amount and location of ice particle impingement.

It is worthwhile to report the definitions and equations used for the particle analysis. These include collection efficiency or impingement efficiency (β), average collection efficiency (β_{ave}), impingement rate (IR), and scoop factor (SF). Impingement efficiency is a non-dimensional measure of the mass flux for a surface and is dependent upon the amount of convergence or dispersion of particles in a flow and the orientation of the surface relative to the particle paths. An impingement efficiency of one means the surface particle flux rate is equal to the free stream particle flux rate. A value less than one means the surface particle flux rate is less than the free stream particle flux rate and a value greater than one means that the surface particle flux rate is greater than the free stream level. The average collection efficiency is defined as:

$$\beta_{avg} = \frac{\sum_{n=1}^{n=N} \beta_n \times A_n}{A_{wetted}} \tag{1}$$

Where N is the number of surface elements with nonzero impingement and β_n, A_n are the collection efficiency and area of surface element n, respectively. The wetted area of the element is the sum of the area of the elements which have non-zero impingement for which we have the equation:

$$A_{wetted} = \sum_{n=1}^{n=N} A_n \tag{2}$$

The impingement rate for a surface is defined as:

$$IR = \beta_{avg} \times LWC_{\infty} \times V_{\infty} \times A_{wetted} \tag{3}$$

Where LWC_{∞} is the free stream liquid water content and V_{∞} is the free stream speed. The free stream catch fraction or scoop factor (SF) is defined as the ratio of the mass impinging on a component divided by the mass available in the free stream for an area equal to the area bounded by the highlight of the inlet lip. The scoop factor is then:

$$SF = \frac{IR}{IR_{\infty}} \tag{4}$$

The free stream impingement rate (IR_{∞}) is defined as the rate at which the particles pass through an area traced out by the highlight of the inlet lip (A_{∞}) traveling at the free stream speed (V_{∞}) with an average collection efficiency of 1 and an LWC matching that of the free stream (LWC_{∞}). The average collection efficiency for a surface is then:

$$\beta_{avg} = \frac{IR \times A_{\infty}}{IR_{\infty} \times A_{wetted}} = SF \times \frac{A_{\infty}}{A_{wetted}} \tag{5}$$

Figure 3 shows the particle impact locations, impingement efficiency, and particle impact temperatures for the 5 μm particle case. From the ice particle trajectory impact points and impingement efficiency shown in Figures 3(a) to (c) we can see that impingement occurs throughout the low pressure compressor. The ice particle trajectory impact point plot (Fig. 3(a)) displays the impact locations for the particles calculated in each of the blocks for the “block-to-block” method. This plot illustrates the density and location of the impacting particles used in the “block-to-block” method (each impact is represented by a red triangle). The engine schematic shown in Figure 1(c) is useful in clarifying the various elements which receive impingement. The peak value of average impingement efficiency for the various surface elements listed in Table 1 was for the inlet lip #1 (0.17). The scoop factors were relatively small for the 5 μm particle for the various surface components shown in Table 1 (<6 percent). The amount of mass entering the inner core was 16.126 g/m^3 which yielded a scoop factor of 0.0679. Figure 3(d) shows the temperature distribution of the impacting particles. As can be seen from the plot the impact temperatures of the particles increase as they pass through the compressor. The lowest impact temperatures from Figure 3(d) are observed on the spinner while the highest were observed on splitter lip #2 and the aft support strut. As the ice particles transport through the warming environment of the engine they increase in temperature and in some cases sublimate or melt and evaporate. The maximum average particle temperature for the 5 μm ice particle was 273.29 K (slightly above the freezing temperature of water) and

occurred on splitter lip #2 (Table 1). From the table we can also so that there was a small amount of melting at the splitter lip #2 because the average melting fraction for splitter lip #2 was less than one (0.836). The melting fraction is defined as the percentage of ice mass to total mass. A melting fraction of one means the particle is totally frozen. A melting fraction of zero means that the particle is totally water. We can also see from Table 1 that there was an appreciable amount of particle sublimation and evaporation for the 5 μm ice particles entering the engine core (~22 percent).

The particle impact, impingement efficiency, and temperature results for the 20 μm particle case are show in Figure 4. As for the 5 μm ice particle the 20 μm ice particle revealed impingement throughout the low pressure compressor although the impingement area was larger for the 20 μm particle (Figs. 3(c) and 4(c)). For most of the components the impingement rates were higher for the 20 μm particle than for the 5 μm particle due to particle inertia (Tables 1 and 2). Larger particles, which have larger inertia, are more resistive to changes in direction due to flow gradients than smaller particles which results in the larger particles being less apt to avoid obstacles. The amount of mass entering the inner core was 10.509 g/m^3 which yielded a scoop factor of 0.0443. The mass entering the core for the 20 μm particle was smaller than for the 5 μm particle because the larger particles were less able to negotiate the turn into the inner core due to their larger inertia. The peak value of average impingement efficiency for the various surface elements listed in Table 2 was for splitter lip #2 (0.3865). The scoop factors were larger for the 20 μm particle than for the 5 μm particle due to particle inertia. The maximum value of scoop factor for the 20 μm particle was for the fan blade (0.3870). From the temperature distributions in Figure 4(d) and Table 2 we see that the maximum average temperature for the 20 μm particle was 270.38 K which occurred on splitter lip #2. This was less than that for the 5 μm particle and is due to the thermal mass of the 20 μm particle being larger and hence more resistive to temperature change. We also see from Table 2 that there was no melting of the 20 μm particle and that there was a very small amount of sublimation for some of the elements.

The particle impact, impingement efficiency, and temperature results for the 100 μm particle case are show in Figure 5. For most of the components the impingement rates were higher for the 100 μm particle than for the 20 and 5 μm particles due to particle inertia (Tables 1 to 3). The amount of mass entering the inner core was 0.181 g/m^3 which yielded a scoop factor of 0.0008. The mass entering the core for the 100 μm particle was smaller than for both the 5 and 20 μm particles because the larger particles were less able to negotiate the turn into the inner core due to their larger inertia. The peak value of average impingement efficiency for the various surface elements listed in Table 3 was for IGV #1 (0.9368). The scoop factors were larger for the 100 μm particle than for the 20 and 5 μm particles due to particle inertia. The maximum value of scoop factor for the 100 μm particle was for the fan blade (0.8248). From the temperature distributions in Figure 5(d) and Table 3 we see that the maximum average temperature for the 100 μm particle was 253.09 K which occurred at the exit of the inner core. This was less than that for the 20 and 5 μm particles and is due to the larger thermal mass of the 100 μm particles. We also see from Table 3 that there was no melting and sublimation of the 100 μm particle for any of the elements.

Conclusion

Predictions for ice particle impingement efficiency, temperature, and melting fraction were generated for the E^3 low pressure compressor using the Glenn Ice Particle Phase Change Model newly incorporated into LEWICE3D Version 3.2 and a flow solution from the ADPAC flow solver. The impingement efficiency results showed that as particle size increased average impingement efficiencies and scoop factors increased for the various components. The particle analysis also showed that the amount of mass entering the core decreased with increased particle size because the larger particles were less able to negotiate the turn into the inner core due to particle inertia. The particle phase change analysis results showed that the larger particles warmed less as they were transported through the low pressure compressor. Only the smallest 5 μm particles were warmed enough to produce melting and the amount of

melting was relatively small with a maximum average melting fraction of 0.836. The results also showed an appreciable amount of particle sublimation and evaporation for the 5 μm particles entering the engine core (22 percent). These results suggest that the newly developed NASA Glenn "block-to-block" icing analysis method can be a useful tool for the analysis of turbomachinery subject to the HIWC environment.

References

1. Mason, J; Strapp, W and Chow, P; "The Ice Particle Threat to Engines in Flight," 44th AIAA Aerospace Sciences Meeting, v4, 2006, pp. 2445-2465.
2. Mazzawy R.S., Strapp J.W.; "Appendix D – An Interim Icing Envelope; SAE 2007-01-3311; *SAE 2007 Aircraft and Engine Icing International Conference*; Seville, Spain, November 2007.
3. Federal Aviation Regulation, Part 25, "Airworthiness Standard: Transport Category Airplanes, Appendix C," DOT, FAA, 1974, rev. 1982.
4. Hamed, A., Das, K., Basu, D., "Numerical Simulations of Ice Droplet Trajectories and Collection Efficiency on Aero-engine Rotating Machinery," AIAA-2005-1248, 2005.
5. Wright, W., Jorgenson, P., Veres, J., "Mixed Phase Modeling in GlennICE with Application to Engine Icing," AIAA-2010-7674, 2010.
6. Bidwell, C., "Particle Trajectory and Icing Analysis of the E^3 Turbofan Engine Using LEWICE3D Version 3," AIAA-2011-38-0048, 2011.
7. Bidwell, C.S., Potapczuk, M.G., "Users Manual for the NASA Lewis Three-Dimensional Ice Accretion Code (LEWICE3D)," NASA TM-105974, December 1993.
8. Cline, S.J., Halter, P.H., Kutney, J.T., and Sullivan, T.J., "Energy Efficient Engine: Fan and Quarter-Stage Component Performance Report," NASA CR 168070, Jan. 1983.
9. Bridgeman, M.J., Cherry, D.G., and Pedersen, J., "NASA/GE Energy Efficient Engine Low Pressure Turbine Scaled Test Vehicle Performance Report," NASA CR 168290, Jul. 1983.
10. Rowe, R.K. and Kuchar, A.P., "Energy Efficient Engine (E 3) Scaled Mixer Performance Report - Final Report," NASA CR 167947, Nov. 1982.
11. Steinbrenner, J.P., Chawner, J.R., Fouts, C.L., "The Gridgen 3D Multiple Block Grid Generation System," Final Report WRDC-TR-90-3022, June 1990.
12. Adamczyk, J.J., Celestina, M.L., and Beach, T.A., "Simulation of Three-Dimensional Viscous Flow Within a Multistage Turbine," ASME Paper 89-GT-152, 1989.
13. Hall, E., Heidegger, N., Delaney, R., "ADPAC v1.0 – Users's Manual," NASA CR 1999-206600.
14. Hall, E., Delaney, R., Lynn, S., Veres, J., "Energy Efficient Low Pressure Subsystem Aerodynamic Analysis," NASA TM 1988-208402.

TABLE 1.—E^3 TRANSPORT STATISTICS FOR AN ICE PARTICLE SIZE OF 5 μm

Element	β_{avg}	Impingement rate, g/s	Scoop factor	D_{avg}, μm	T_{avg}, K	Melt Fraction$_{avg}$
Free stream capture tube[a]	1.0000	237.397	1.0000	5.00	229.30	1.00
Inlet lip	0.1746	2.353	0.0099	4.94	255.75	1.00
Inlet capture	0.8640	183.956	0.7749	4.94	239.40	1.00
Spinner	0.0927	1.020	0.0043	4.89	255.90	1.00
Fan blade	0.0432	12.702	0.0535	4.85	262.95	0.986
Splitter lip #1	0.0856	1.150	0.0048	4.87	267.10	0.987
IGV #1	0.0913	3.523	0.0148	4.69	269.55	0.931
Rotor #1	0.0744	1.955	0.0082	4.80	270.92	0.864
Splitter lip #2	0.1427	0.825	0.0035	4.64	273.29	0.836
Inner core	0.6965	16.126	0.0679	4.61	271.99	0.952

[a]Based on capture area of 3.26 m^2

TABLE 2.—E^3 TRANSPORT STATISTICS FOR AN ICE PARTICLE SIZE OF 20 μm

Element	β_{avg}	Impingement rate, g/s	Scoop factor	D_{avg}, μm	T_{avg}, K	Melt Fraction$_{avg}$
Free stream capture tube[a]	1.0000	237.397	1.0000	20.00	229.30	1.00
Inlet lip	0.2249	24.402	0.1028	19.99	245.44	1.00
Inlet capture	0.9572	200.823	0.8459	19.98	238.64	1.00
Spinner	0.0803	4.606	0.0194	19.97	250.05	1.00
Fan blade	0.2613	91.862	0.3870	19.97	250.76	1.00
Splitter lip #1	0.1623	5.318	0.0224	19.97	257.26	1.00
IGV #1	0.2768	13.619	0.0574	19.97	253.04	1.00
Rotor #1	0.2639	8.590	0.0362	19.97	260.16	1.00
Splitter lip #2	0.3865	16.317	0.0687	19.92	270.38	1.00
Inner core	1.1958	10.509	0.0443	19.87	270.25	1.00

[a]Based on capture area of 3.26 m^2

TABLE 3.—E^3 TRANSPORT STATISTICS FOR AN ICE PARTICLE SIZE OF 100 μm

Element	β_{avg}	Impingement rate, g/s	Scoop factor	D_{avg}, μm	T_{avg}, K	Melt Fraction$_{avg}$
Free stream capture tube[a]	1.0000	237.397	1.0000	100.00	229.30	1.00
Inlet lip	0.1820	83.816	0.3531	100.00	231.80	1.00
Inlet capture	1.0905	228.779	0.9637	100.00	232.92	1.00
Spinner	0.4085	28.000	0.1179	100.00	236.40	1.00
Fan blade	0.5460	195.799	0.8248	100.00	237.07	1.00
Splitter lip #1	2.1945	76.510	0.3223	100.01	239.88	1.00
IGV #1	0.9368	98.418	0.4146	100.01	239.44	1.00
Rotor #1	0.9171	41.943	0.1767	100.01	241.50	1.00
Splitter lip #2	0.0341	1.395	0.0059	100.03	250.87	1.00
Inner core	0.0078	0.181	0.0008	100.03	253.09	1.00

[a]Based on capture area of 3.26 m^2

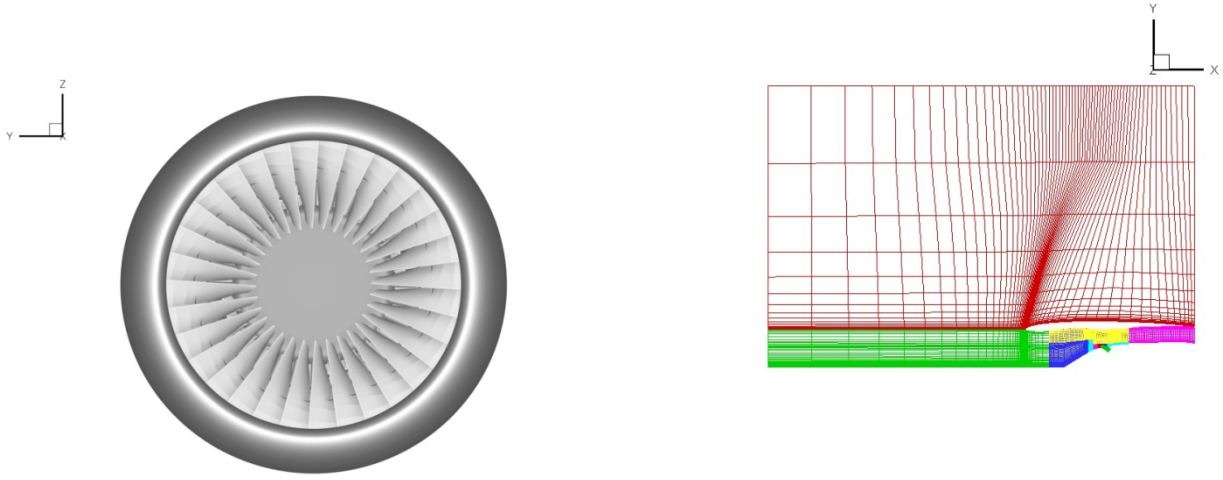

(a) Surface model.

(b) Grid block structure.

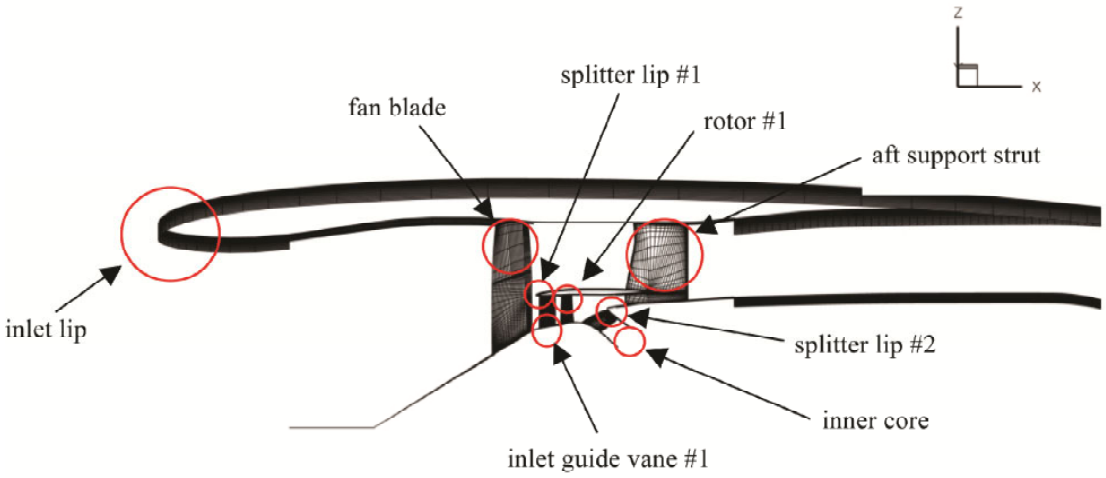

(c) Element designation.

Figure 1.—Surface model and grid structure for E^3 flow model.

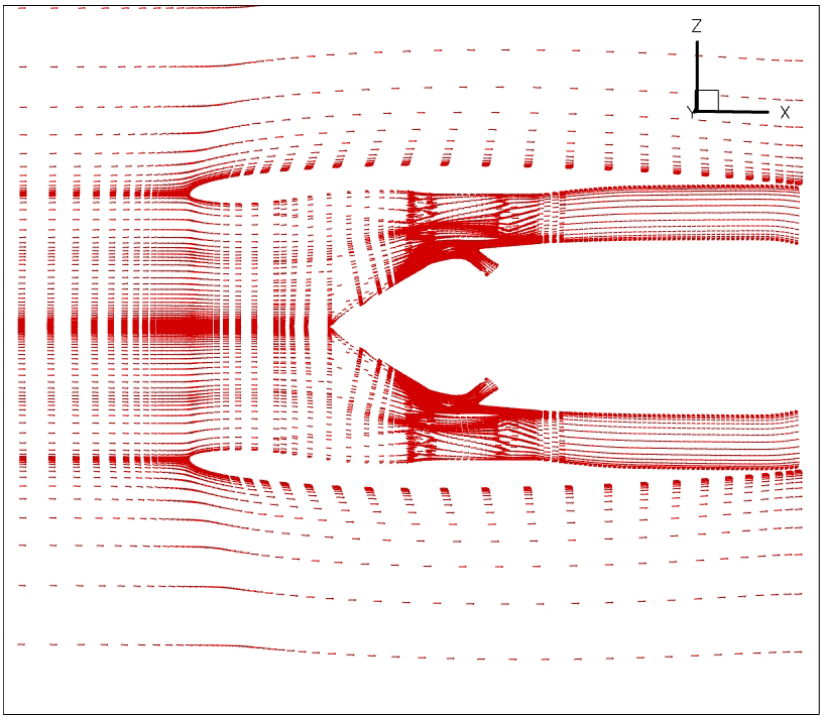

(a) Side view.

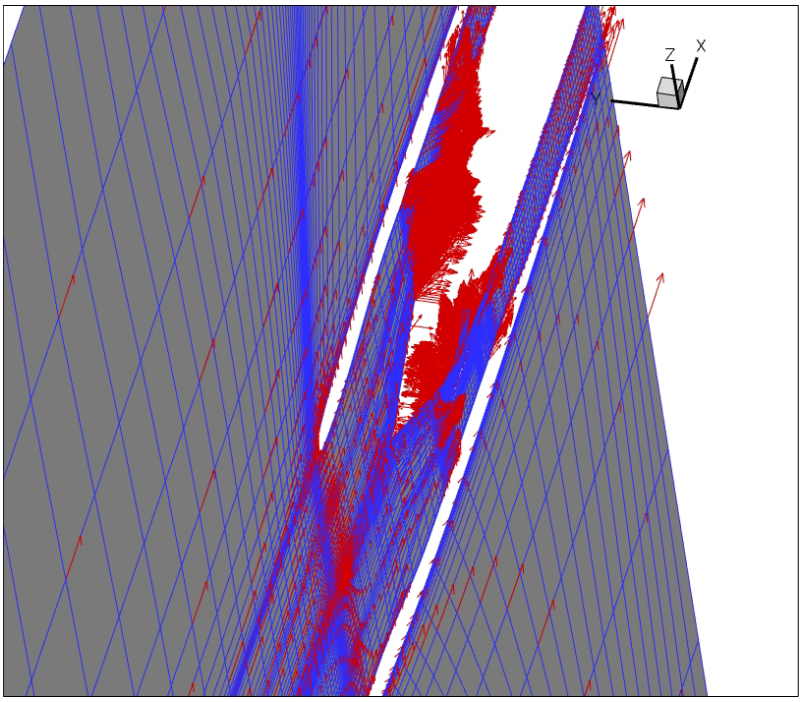

(b) Orthogonal view.

Figure 2.—Centerline velocity vectors for the E^3 low pressure compressor.

(a) Particle impact locations (axial view).

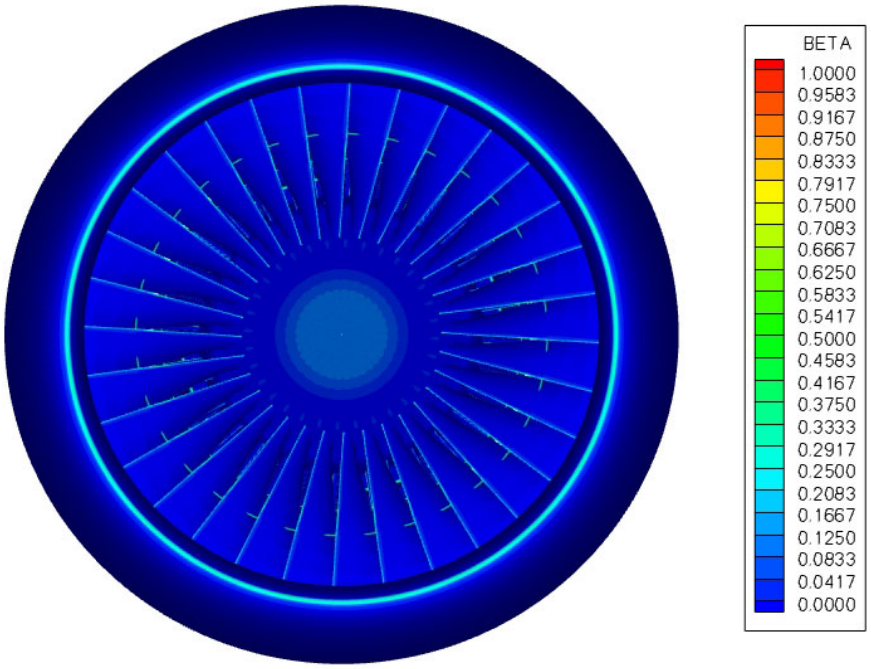

(b) Impingement efficiency.

Figure 3.—E^3 particle transport results for a 5 μm ice particle.

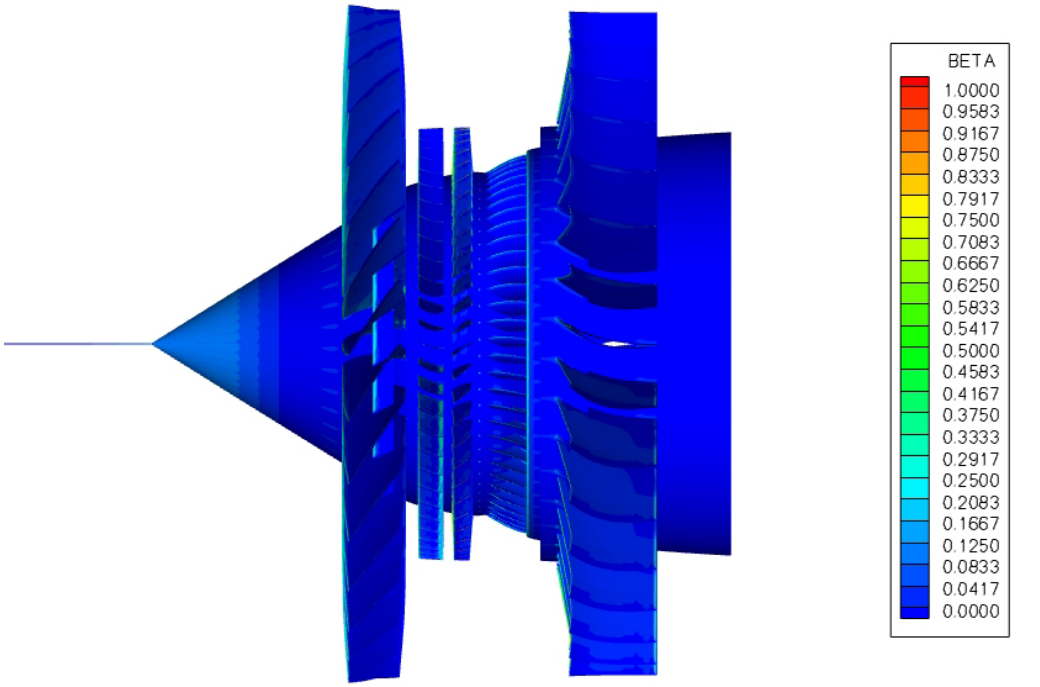

(c) Impingement efficiency (axial view).

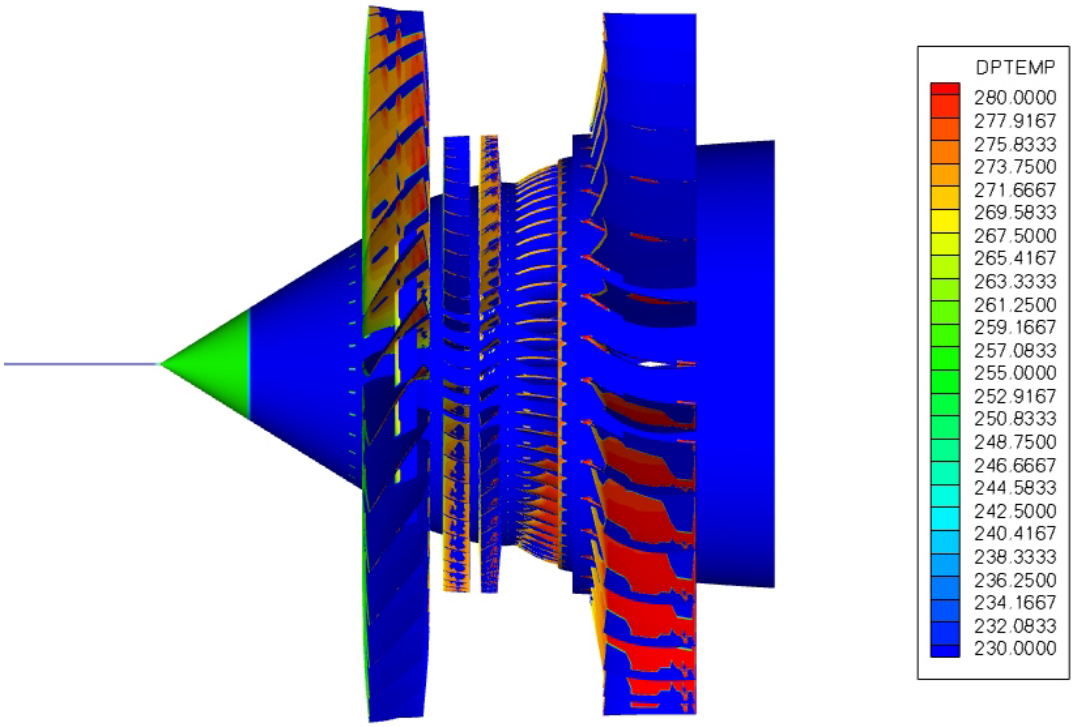

(d) Particle impact temperature.

Figure 3.—Concluded.

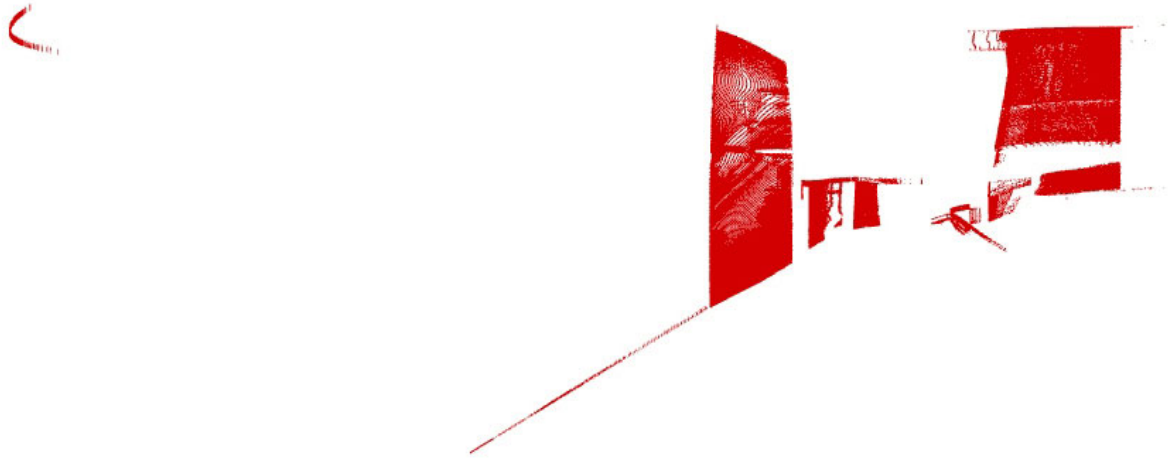

(a) Particle impact locations (axial view).

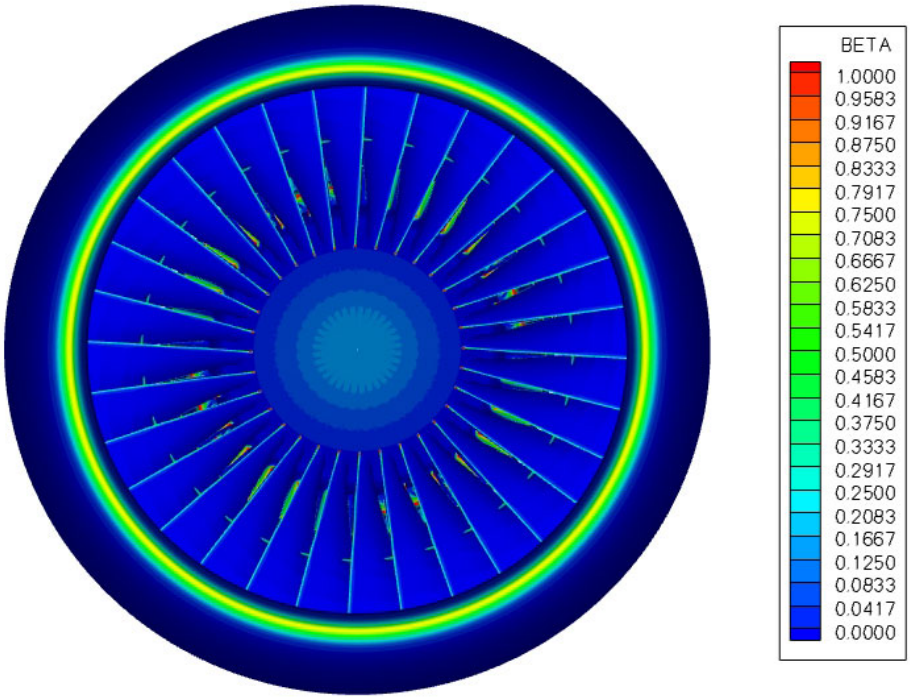

(b) Impingement efficiency.

Figure 4.—E^3 particle transport results for a 20 μm ice particle.

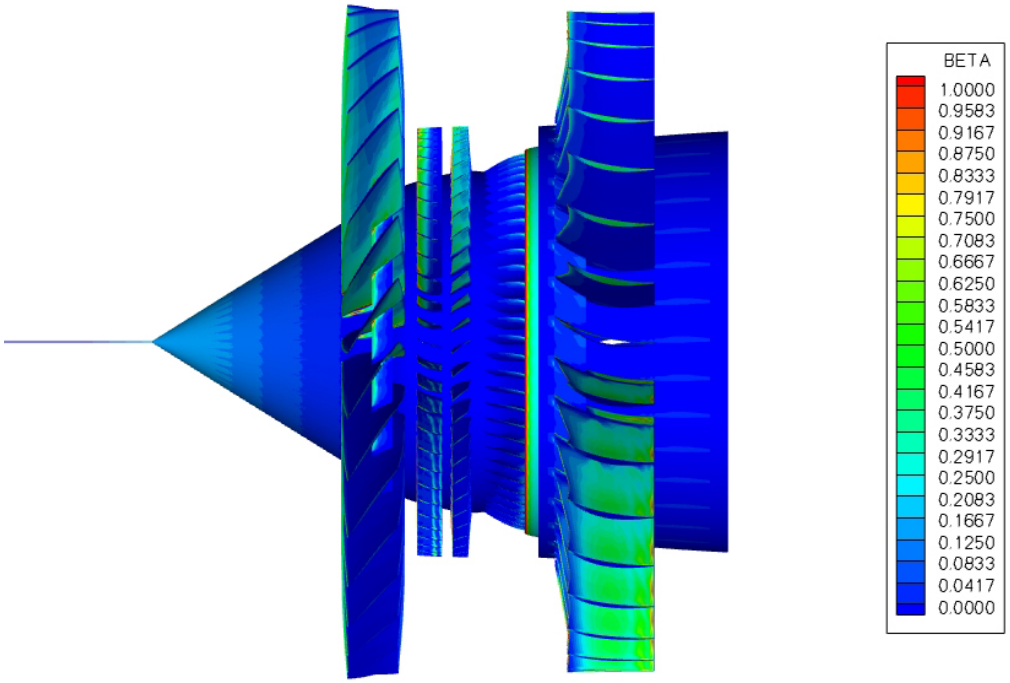

(c) Impingement efficiency (axial view).

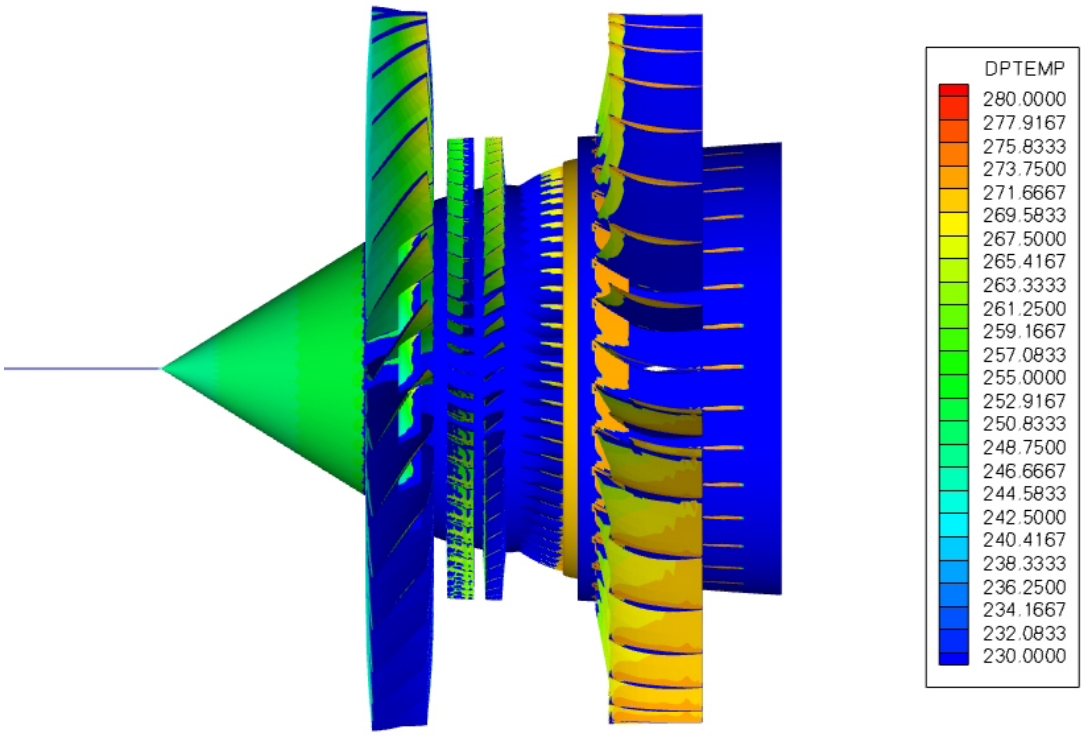

(d) Particle impact temperature.

Figure 4.—Concluded.

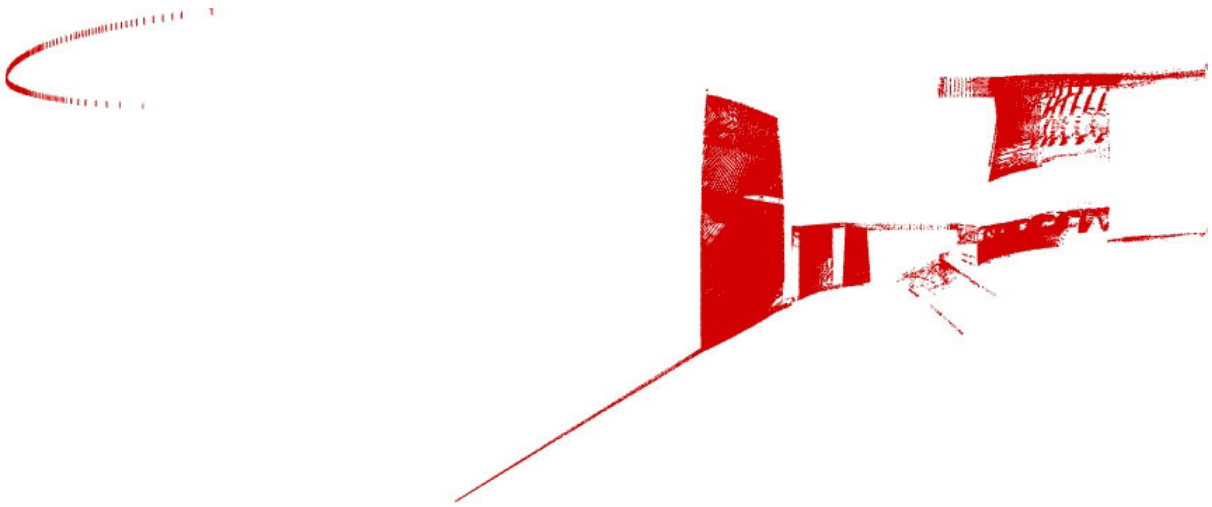

(a) Particle impact locations (axial view).

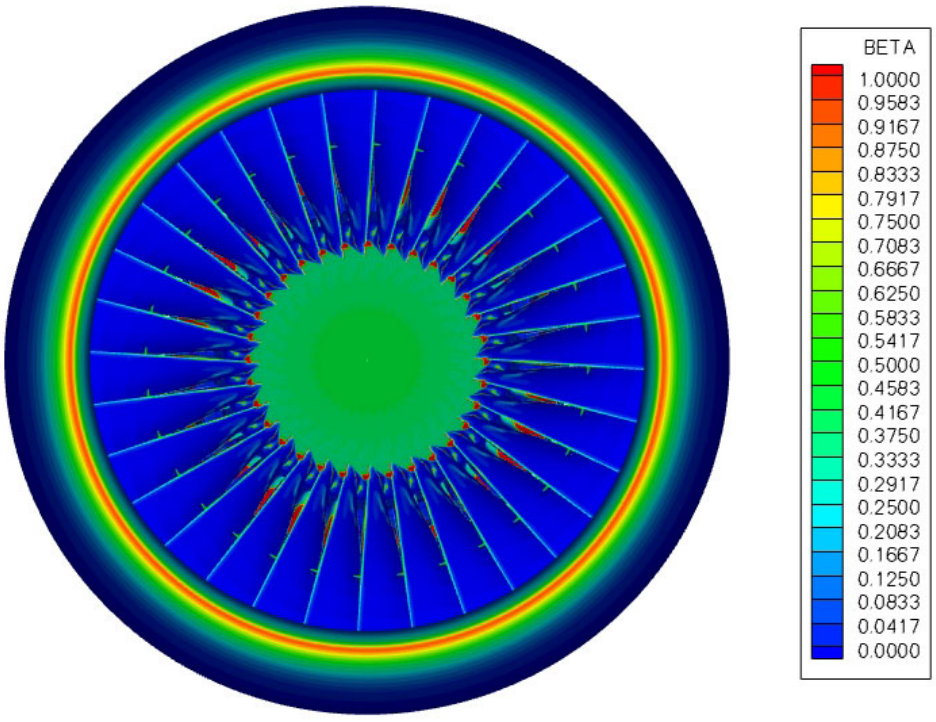

(b) Impingement efficiency.

Figure 5.—E^3 particle transport results for a 100 μm ice particle.

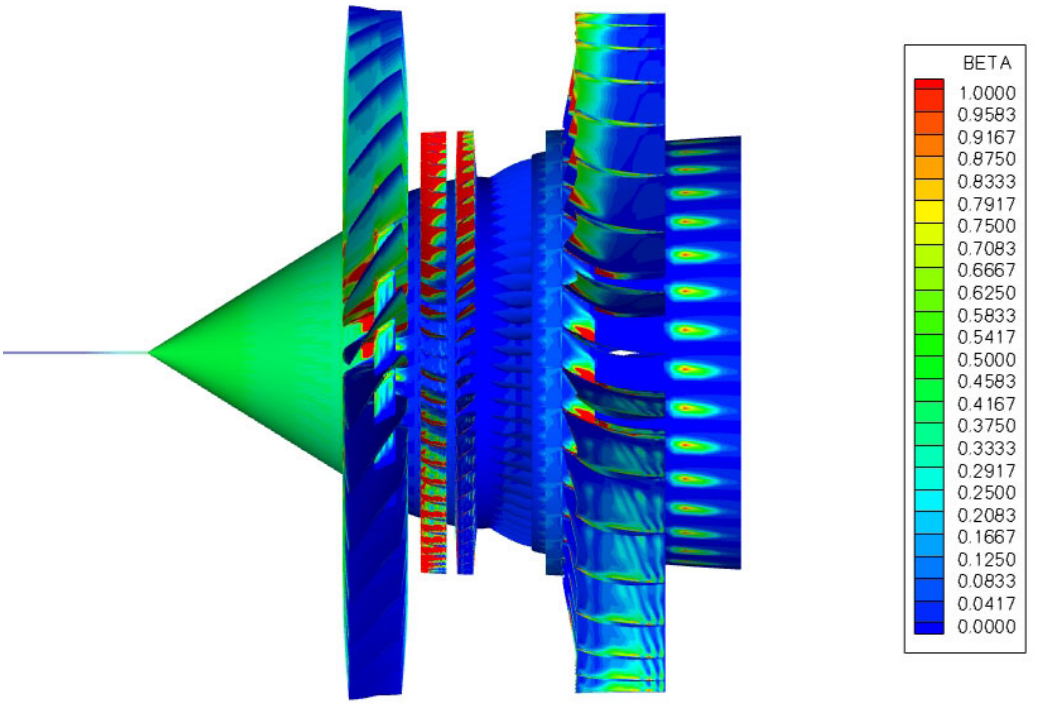

(c) Impingement efficiency (axial view).

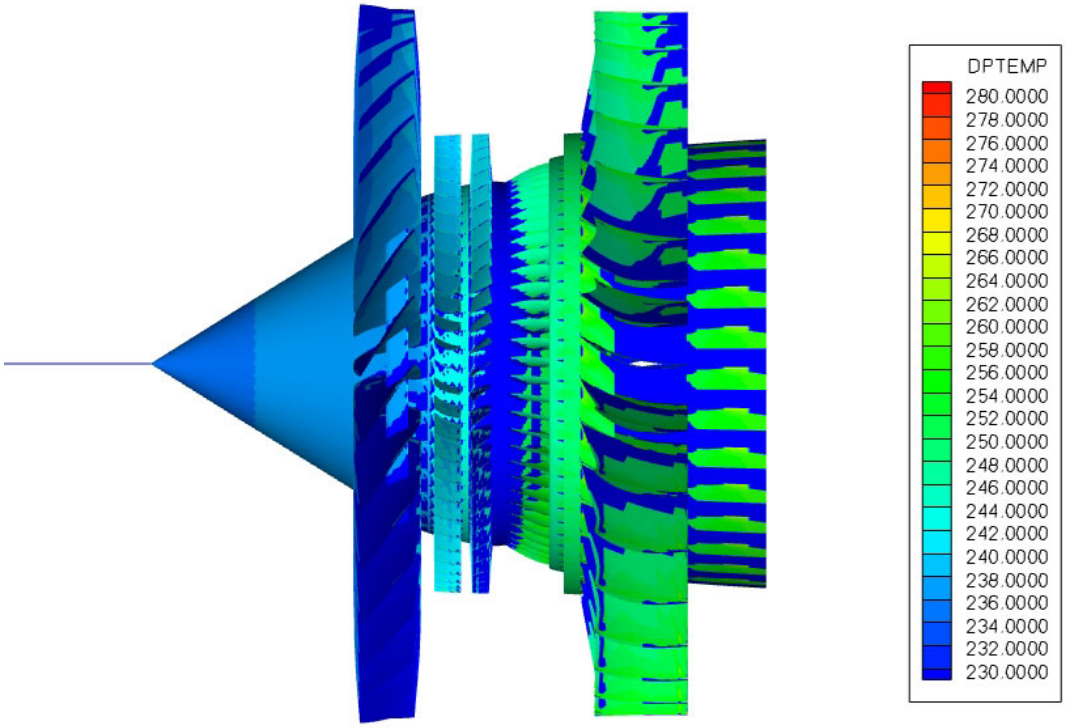

(d) Particle impact temperature.

Figure 5.—Concluded.

REPORT DOCUMENTATION PAGE	Form Approved OMB No. 0704-0188

1. REPORT DATE *(DD-MM-YYYY)*	2. REPORT TYPE	3. DATES COVERED *(From - To)*
01-09-2012	Technical Memorandum	

4. TITLE AND SUBTITLE
Ice Particle Transport Analysis With Phase Change for the E^3 Turbofan Engine Using LEWICE3D Version 3.2

5a. CONTRACT NUMBER

5b. GRANT NUMBER

5c. PROGRAM ELEMENT NUMBER

6. AUTHOR(S)
Bidwell, Colin, S.

5d. PROJECT NUMBER

5e. TASK NUMBER

5f. WORK UNIT NUMBER
WBS 648987.02.02.03.20

7. PERFORMING ORGANIZATION NAME(S) AND ADDRESS(ES)
National Aeronautics and Space Administration
John H. Glenn Research Center at Lewis Field
Cleveland, Ohio 44135-3191

8. PERFORMING ORGANIZATION REPORT NUMBER
E-18387

9. SPONSORING/MONITORING AGENCY NAME(S) AND ADDRESS(ES)
National Aeronautics and Space Administration
Washington, DC 20546-0001

10. SPONSORING/MONITOR'S ACRONYM(S)
NASA

11. SPONSORING/MONITORING REPORT NUMBER
NASA/TM-2012-217700

12. DISTRIBUTION/AVAILABILITY STATEMENT
Unclassified-Unlimited
Subject Category: 03
Available electronically at http://www.sti.nasa.gov
This publication is available from the NASA Center for AeroSpace Information, 443-757-5802

13. SUPPLEMENTARY NOTES

14. ABSTRACT
Ice Particle trajectory calculations with phase change were made for the Energy Efficient Engine (E^3) using the LEWICE3D Version 3.2 software. The particle trajectory computations were performed using the new Glenn Ice Particle Phase Change Model which has been incorporated into the LEWICE3D Version 3.2 software. The E^3 was developed by NASA and GE in the early 1980's as a technology demonstrator and is representative of a modern high bypass turbofan engine. The E^3 flow field was calculated using the NASA Glenn ADPAC turbomachinery flow solver. Computations were performed for the low pressure compressor of the E^3 for a Mach 0.8 cruise condition at 11,887 m assuming a standard warm day for ice particle sizes of 5, 20, and 100 μm and a free stream particle concentration of 0.3 g/m^3. The impingement efficiency results showed that as particle size increased average impingement efficiencies and scoop factors increased for the various components. The particle analysis also showed that the amount of mass entering the inner core decreased with increased particle size because the larger particles were less able to negotiate the turn into the inner core due to particle inertia. The particle phase change analysis results showed that the larger particles warmed less as they were transported through the low pressure compressor. Only the smallest 5 μm particles were warmed enough to produce melting and the amount of melting was relatively small with a maximum average melting fraction of 0.836. The results also showed an appreciable amount of particle sublimation and evaporation for the 5 μm particles entering the engine core (22 percent).

15. SUBJECT TERMS
Aircraft icing; Ice crystal particle trajectories; Engine icing

16. SECURITY CLASSIFICATION OF:			17. LIMITATION OF ABSTRACT	18. NUMBER OF PAGES	19a. NAME OF RESPONSIBLE PERSON
a. REPORT	b. ABSTRACT	c. THIS PAGE			STI Help Desk (email:help@sti.nasa.gov)
U	U	U	UU	22	19b. TELEPHONE NUMBER *(include area code)* 443-757-5802